

Exciton Storage in a Nanoscale Aharonov-Bohm Ring with Electric Field Tuning

Andrea M. Fischer,¹ Vivaldo L. Campo, Jr.,² Mikhail E. Portnoi,³ and Rudolf A. Römer¹

¹*Department of Physics and Centre for Scientific Computing, University of Warwick, Coventry, CV4 7AL, United Kingdom*

²*Departamento de Física, Universidade Federal de São Carlos–UFSCar, 13565-905 São Carlos, SP, Brazil*

³*School of Physics, University of Exeter, Exeter EX4 4QL, United Kingdom*

(Received 22 September 2008; published 4 March 2009)

We study analytically the optical properties of a simple model for an electron-hole pair on a ring subjected to perpendicular magnetic flux and in-plane electric field. We show how to tune this excitonic system from optically active to optically dark as a function of these external fields. Our results offer a simple mechanism for exciton storage and readout.

DOI: 10.1103/PhysRevLett.102.096405

PACS numbers: 71.35.Cc, 03.65.Ge

The manipulation of light and excitons is an area which has sparked much recent interest [1–5]. The speed of light has been slowed down to an amazing 17 ms^{-1} in an ultra-cold gas of sodium atoms [2] by the use of electromagnetically induced transparency techniques [6]. Bose-Einstein condensation of an excitonic gas is a phenomenon considered theoretically a long time ago [7]. However, it is only recently that the ability to grow high quality layered semiconductor structures has allowed for a successful experimental investigation of excitonic superfluids. Spatial patterns in photoluminescence measurements of an exciton gas in GaAs/AlGaAs coupled quantum wells have been observed [8] and are thought to be a signature of quantum degeneracy [9]. Zero Hall voltages measured in bilayer quantum-well systems for particular layer separations and magnitudes of a magnetic field applied perpendicular to the layers are also understood to indicate the presence of an excitonic condensate [10]. There has also been experimental evidence for the formation of a polariton Bose-Einstein condensate [11] and a room temperature polariton laser [12]. Such discoveries are very important for quantum computing applications [13]. In current computers, electrons are used for information processing and photons for communication. Conversion between the two media places limitations upon the machine's efficiency. The creation of an exciton-based integrated circuit [14] could provide an exciting solution to this problem. The possibility of using excitons for data storage has also been investigated using indirect excitons in self-assembled quantum dots [3] and coupled quantum wells [1]. Here the electron and hole are separated using a gate voltage, significantly prolonging their lifetimes.

In this Letter we find a mechanism for controlling excitonic lifetimes in a single Aharonov-Bohm (AB) nanoring, again by the use of a constant electric field. Suppression of ground state exciton emission has already been seen for polarized excitons in the ring geometry for particular magnetic field strengths [15]; the introduction of impurities [16,17] and the use of slightly eccentric rings [18] makes previously dark states become optically active.

In the present system, recombination of the electron-hole pair is not prevented by their confinement to different nanostructures, as previously seen, but by appropriate tuning of external magnetic and electric fields. In Fig. 1, we show the oscillator strength F of an exciton in a one-dimensional ring geometry threaded by a perpendicular magnetic flux Φ and in the presence of an in-plane electric field. The oscillator strength oscillates as a function of magnetic flux. The most striking feature, however, is the way these oscillations change as the (dimensionless) electric field u_0 is varied. Up to a certain critical value of u_0 , F peaks at $\Phi = 0.5$ (in units of the universal flux quantum h/e) indicating optimal conditions for the exciton creation and recombination. However, beyond this critical value, F reaches zero at $\Phi = 0.5$ and such transitions are forbidden. The critical electric field strength u_c is comparable to the electron-hole interaction strength v_0 and the transition occurs between $u_0 = 0.3$ and $u_0 = 0.4$ for the value used in Fig. 1. This suggests a mechanism for controlling

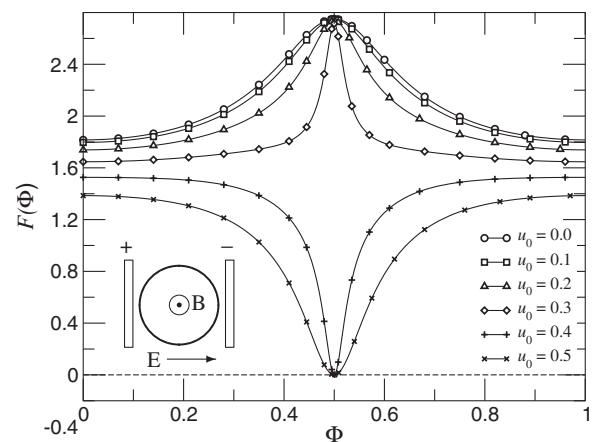


FIG. 1. Oscillator strength F as a function of Φ for electron-hole interaction strength $v_0 = -2/\pi^2$ and various values of the electric field u_0 . The horizontal dashed line indicates $F = 0$. Only every sixth data point is shown for clarity in each curve. Inset: Schematics of the ring geometry and the external fields.

whether an excitonic state is optically active or not and thus whether an exciton is present or absent from the ring. The procedure is (i) begin with $\Phi = 0$ and $u_0 = 0$, (ii) increase the flux adiabatically to $\Phi = 0.5$ so an exciton can easily be created from the vacuum, (iii) decrease Φ , (iv) increase u_0 until it appreciably exceeds the critical value, (v) increase flux to $\Phi = 0.5$. The oscillator strength is now zero, so the exciton is trapped and unable to decay until the external fields are further tuned. This has important implications for excitonic data storage as we shall discuss later.

We study the excitonic ground state energies, wave functions, and corresponding oscillator strengths exactly for the case of a contact electron-hole interaction. We obtain the excitonic wave function as a linear combination of the electron and hole single-particle wave functions, $\psi_N^{(e)}(\theta_e)$ and $\psi_{N'}^{(h)}(\theta_h)$,

$$\Psi(\theta_e, \theta_h) = \sum_{N, N'} A_{NN'} \psi_N^{(e)}(\theta_e) \psi_{N'}^{(h)}(\theta_h), \quad (1)$$

depending on the azimuthal coordinates, θ_e and θ_h , of the electron and hole, respectively. Here, the single-particle electron wave function obeys the dimensionless Schrödinger equation

$$\begin{aligned} \mathbf{H}(u_0, \Phi) \psi^{(e)}(\theta_e) &= \lambda^{(e)} \psi^{(e)}(\theta_e) \\ &\equiv \left[-\frac{d^2}{d\theta_e^2} + 2i\Phi \frac{d}{d\theta_e} + \Phi^2 \right. \\ &\quad \left. - u_0 \cos(\theta_e) \right] \psi^{(e)}(\theta_e), \end{aligned} \quad (2)$$

where $\Phi = -\rho A e / \hbar$, $u_0 = e \rho U_0 / \epsilon_0$, $\lambda^{(e)} = E_e / \epsilon_0$, and $\epsilon_0 = \hbar^2 / 2m_e \rho^2$, and ρ is the ring radius, A the magnetic vector potential, U_0 the constant in-plane electric field, E_e the energy of the electron, and m_e the mass of the electron. The Schrödinger equation is the same for the hole aside from a change in sign for Φ and u_0 . The eigensolutions of (2), a Mathieu equation with external flux [19], can be constructed by Fourier expansion of the single-particle wave functions and obtaining the expansion coefficients and energies from the resulting matrix eigenequation.

The Hamiltonian for the two particle excitonic system is given by $\mathbf{H}(u_0, \Phi) + \mu \mathbf{H}(-u_0/\mu, -\Phi) + V[R(\theta_e - \theta_h)]$, where $\mu = m_e/m_h$ is the ratio of the electron and hole masses [20] and V is the interaction term, which depends on the distance R between the electron and hole. We assume a short range interaction $V[R(\theta_e - \theta_h)]/\epsilon_0 = 2\pi v_0 \delta(\theta_e - \theta_h)$, where v_0 is the average interaction strength in units of ϵ_0 . v_0 is chosen as multiples of $-1/\pi^2$, so that the spatial extent of the exciton is comparable to the ring circumference, ensuring an appreciable AB effect [21]. The Schrödinger equation may now be written as

$$\begin{aligned} \sum_{N, N'} A_{NN'} (\lambda_N^{(e)} + \lambda_{N'}^{(h)} - \Delta) \psi_N^{(e)}(\theta_e) \psi_{N'}^{(h)}(\theta_h) \\ + 2\pi v_0 \delta(\theta_e - \theta_h) \Psi(\theta_e, \theta_h) = 0, \end{aligned} \quad (3)$$

where Δ is the excitonic energy in units of ϵ_0 . Multiplying by $[\psi_N^{(e)}(\theta_e) \psi_{N'}^{(h)}(\theta_h)]^\dagger$ for particular $N, N' \in \mathbb{Z}$ and integrating over $\theta_e, \theta_h \in [0, 2\pi]$ allows us to obtain an expression for the coefficients in Eq. (1)

$$\begin{aligned} A_{NN'} &= -\frac{2\pi v_0}{\lambda_N^{(e)} + \lambda_{N'}^{(h)} - \Delta} \\ &\quad \times \int_0^{2\pi} d\theta \Psi(\theta, \theta) \psi_{N'}^{(h)}(\theta)^\dagger \psi_N^{(e)}(\theta)^\dagger. \end{aligned} \quad (4)$$

Multiplying Eq. (1) with $\theta_e = \theta_h = \theta$ by $\psi_{N'_0}^{(h)}(\theta)^\dagger \psi_{N_0}^{(e)}(\theta)^\dagger$ and integrating over $\theta \in [0, 2\pi]$ gives

$$\begin{aligned} \int_0^{2\pi} d\theta \Psi(\theta, \theta) \psi_{N'_0}^{(h)}(\theta)^\dagger \psi_{N_0}^{(e)}(\theta)^\dagger \\ = \sum_{N, N'} A_{NN'} \int_0^{2\pi} d\theta \psi_N^{(e)}(\theta) \psi_{N'}^{(h)}(\theta) \psi_{N'_0}^{(h)}(\theta)^\dagger \psi_{N_0}^{(e)}(\theta)^\dagger. \end{aligned} \quad (5)$$

Let

$$\begin{aligned} P_{NN'N_0N'_0} &= -\frac{2\pi v_0}{\lambda_N^{(e)} + \lambda_{N'}^{(h)} - \Delta} \\ &\quad \times \int_0^{2\pi} d\theta \psi_N^{(e)}(\theta) \psi_{N'}^{(h)}(\theta) \psi_{N'_0}^{(h)\dagger}(\theta) \psi_{N_0}^{(e)\dagger}(\theta) \end{aligned} \quad (6)$$

and

$$G_{NN'} = \int_0^{2\pi} d\theta \Psi(\theta, \theta) \psi_{N'}^{(h)\dagger}(\theta) \psi_N^{(e)\dagger}(\theta). \quad (7)$$

Then Eq. (5) can be expressed as

$$G_{N_0N'_0} = \sum_{N, N'} G_{NN'} P_{NN'N_0N'_0}(\Delta). \quad (8)$$

No analytic solution of (8) is known for finite v_0 and u_0 [21]. In order to find approximate solutions to (8), we cut off the sums at a maximum value N_{\max} for N, N', N_0, N'_0 . We have chosen $N_{\max} = 15$ for calculation of the excitonic energies and $N_{\max} = 11$ for the oscillator strengths; we have tested that our results do not change appreciably for the range of Φ , u_0 , and v_0 considered here. Mapping $N, N' \rightarrow K$ and $N_0, N'_0 \rightarrow K_0$ according to $K = (N-1)N_{\max} + N'$, allows Eq. (8) to be reformulated as a standard matrix equation $G_{K_0} = \sum_K G_K P_{KK_0}(\Delta)$. The excitonic energies may now be calculated numerically by determining the values of Δ which result in the matrix P_{KK_0} having an eigenvalue equal to 1. For given Δ , all eigenstates can be found using (7), (4), and (1).

Figure 2 shows the resulting excitonic energies plotted as a function of magnetic flux for different electric field strengths. For small enough finite electric fields, the exci-

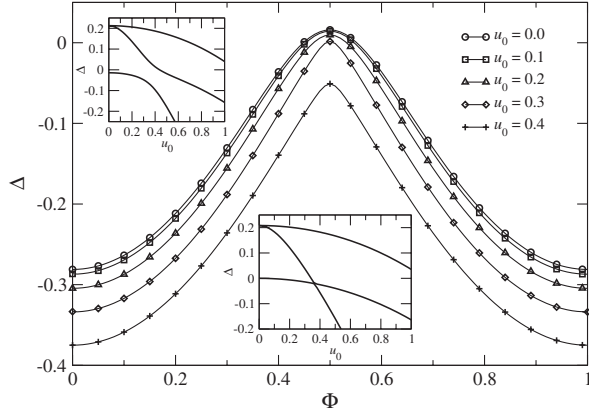


FIG. 2. Excitonic energy as a function of magnetic flux Φ at various values of electric field u_0 for interaction strength $v_0 = -2/\pi^2$. Only every fourth data point is shown for clarity in each curve. Top inset: The energies of the first three states at $\Phi = 0.45$ as a function of u_0 . Bottom inset: The first three states at $\Phi = 0.5$ as a function of u_0 .

tonic energy oscillates as a function of the magnetic field as seen previously for $u_0 = 0$ [21]. This is due to the electron and hole, which were created simultaneously at the same position, having a finite probability to tunnel in opposite directions and meet each other on the opposite side of the ring. The dependence of the oscillation amplitude upon electric field strength is shown in Fig. 3 for different values of the interaction strength. In all cases there is initially a small increase [22] in amplitude $\Delta(\Phi = 0.5) - \Delta(\Phi = 0.0)$ and then it decreases strongly as a function of electric field strength. This change happens when the polarization energy $2u_0$ becomes comparable to the exciton binding energy, which is $\pi^2 v_0^2/2$ on a line. As seen in the inset of Fig. 3, the polarization energy should be calculated with

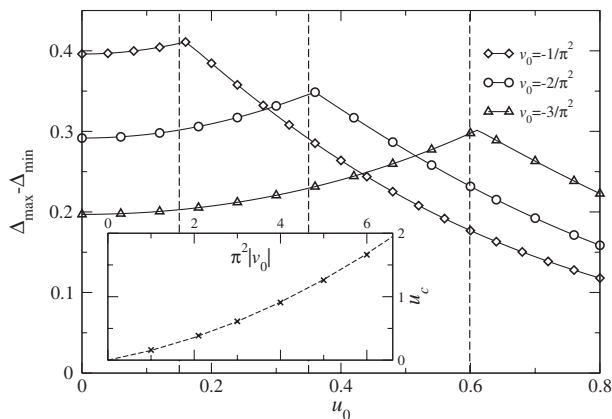


FIG. 3. Amplitude of the Aharonov-Bohm oscillations as a function of external field u_0 at various values of the interaction strength v_0 . Only every sixth data point is shown. Inset: Critical external field u_c as a function of v_0 . The dashed curve, $u_c = \pi|v_0|/(\pi|v_0|/4 + 2/5)$, fits the numerical points quite well. The vertical dashed lines in the main plot indicate $u_c(v_0)$.

an effective electric field, E_{eff} , where $eE_{\text{eff}}R/\epsilon_0 = u_0 - 2\pi v_0/5$. More precisely, the change of behavior corresponds to a level crossing between ground and first excited state which only occurs at $\Phi = 0.5$ as shown in the insets of Fig. 2 [23]. The level crossing is associated with an exact symmetry at $\Phi = 0.5$ upon exchanging $\theta_{e,h} \rightarrow -\theta_{e,h}$. The quadratic behavior for small enough magnetic fluxes and the negative curvature of Δ are as expected from second order perturbation theory in u_0 as shown in Fig. 4. For magnetic flux values close to $\Phi = 0.5$, the excitonic energy remains almost constant as a function of electric field until the critical u_0 value, when the level crossing occurs.

The oscillator strength $F = |\int_0^{2\pi} d\theta \Psi(\theta, \theta)|^2 / \int_0^{2\pi} d\theta_e \int_0^{2\pi} d\theta_h |\Psi(\theta_e, \theta_h)|^2$ was already shown in Fig. 1 as a function of magnetic flux Φ for various values of electric field strength. It measures the strength of a transition from the ground state $\Psi(\theta_e, \theta_h)$ into the vacuum state. We note that the transition from optically active to dark coincides with the change in slope of the amplitude of the excitonic AB oscillation as in Fig. 3 and also the reinstatement of the parabolic behavior in Fig. 4. In order to explain the mechanism for this behavior, we show in Fig. 5 the probability density function for the exciton at different values of Φ , u_0 , and v_0 . In Fig. 5(a) the magnetic flux and electric field have been set to zero. The dark gray diagonal region indicates a peak in probability density where the electron and hole coordinates are close together, so the exciton is very small. In Fig. 5(b) the flux has been increased from its zero value, while keeping the interaction strength and electric field constant. There is a slight narrowing of the peaked region and the contours are closer together, showing that the exciton has become smaller. In Fig. 5(c) the magnetic flux and interaction strength are the same as in Fig. 5(a), but the electric field has been increased. We see the dark gray region has begun to split in two, suggesting the exciton is beginning to separate. In

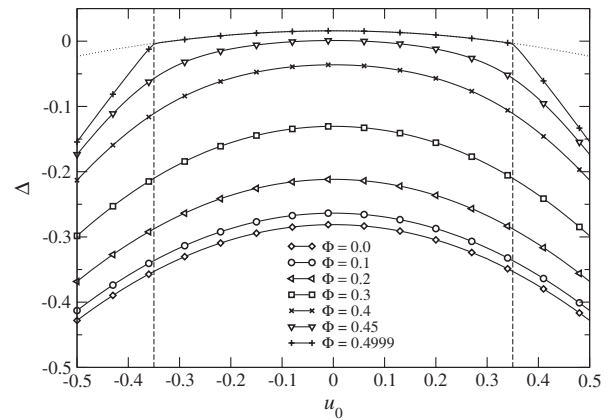


FIG. 4. Excitonic energy as a function of u_0 for interaction strength $v_0 = -2/\pi^2$ and various values of Φ . Only every sixth data point is shown. The dotted lines show the results of second order perturbation theory performed on the ground state. The vertical dashed lines indicate u_c .

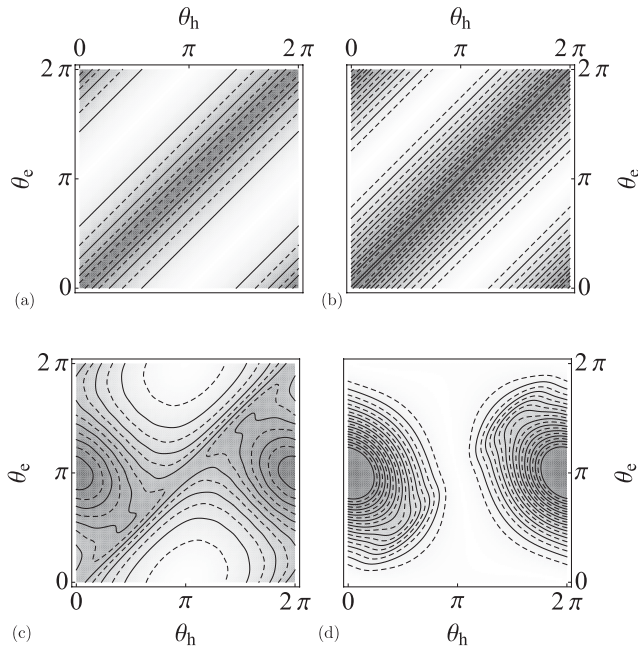


FIG. 5. Excitonic probability density $|\Psi(\theta_e, \theta_h)|^2$ at $\nu_0 = -2/\pi^2$ and (a) $u_0 = 0$, $\Phi = 0$, (b) $u_0 = 0$, $\Phi = 0.4999$, (c) $u_0 = 0.5$, $\Phi = 0$, and (d) $u_0 = 0.5$, $\Phi = 0.4999$. The solid lines and dashed lines are contour lines separated in height by $1/10\pi^2$.

Fig. 5(d) the magnetic flux has been increased from its zero value in Fig. 5(c). The result is two dark gray peaks indicating that the exciton has been broken [3] into an electron and hole, which are located on opposite sides of the ring.

In conclusion, we have presented a simple model which allows the tuning of an exciton from light to dark by the application of external fields similar to previous experiments in quantum dots [3]. Rings of InAs drops with radius $\lesssim 50$ nm on GaAs surfaces have been fabricated [24]. The important feature is that the overall sensitivity can be optimized with the external magnetic field, while the control can be achieved with simple local electric gates. Moderate magnetic fields of a few Tesla as well as an electric field of ~ 100 V/cm would be sufficient to observe the proposed effects for such a ring at moderately low temperatures of the order of 10 K. This suggests that our model might be useful in the quest to trap and store light [1–3,14]. Also, the contrast $F(u_0 = 0)/F(u_0 \gg 0)$ at $\Phi = 0.5$ remains much more pronounced in larger rings than that of the ground state energy AB oscillations. Hence we expect that the effect is visible in somewhat larger rings and in the presence of weak impurities.

We gratefully acknowledge discussions with M. Bergin, A. Chaplik, A. Pennycook, G. Rowlands, and S. A. Wells. A.M.F. and R.A.R. thank EPSRC and the Nuffield Foundation for funding. M.E.P., R.A.R., and V.L.C. are grateful for hospitality at the International Centre for

Condensed Matter Physics (Brasilia) where part of this work was done.

-
- [1] A. Winbow, A. Hammack, and L. V. Butov, *Nano Lett.* **7**, 1349 (2007).
 - [2] L. V. Hau, S. Harris, Z. Dutton, and C. Behroozi, *Nature (London)* **397**, 594 (1999).
 - [3] T. Lundstrom, W. Schoenfeld, H. Lee, and P. Petroff, *Science* **286**, 2312 (1999).
 - [4] L. V. Butov, *J. Phys. Condens. Matter* **19**, 295202 (2007).
 - [5] Y. Mitsumori, T. Kuroda, and F. Minami, *J. Lumin.* **87–89**, 914 (2000).
 - [6] S. Harris, J. Field, and A. Imamoglu, *Phys. Rev. Lett.* **64**, 1107 (1990).
 - [7] L. V. Keldysh and Yu. V. Kopaev, *Fiz. Tverd. Tela (Leningrad)* **6**, 2791 (1964) [*Sov. Phys. Solid State* **6**, 2219 (1965)].
 - [8] L. V. Butov, A. Gossard, and D. Chemia, *Nature (London)* **418**, 751 (2002).
 - [9] L. Levitov, B. Simons, and L. V. Butov, *Phys. Rev. Lett.* **94**, 176404 (2005).
 - [10] M. Kellogg, J. Eisenstein, L. Pfeiffer, and K. West, *Phys. Rev. Lett.* **93**, 036801 (2004); E. Tutuc, M. Shayegan, and D. Huse, *Phys. Rev. Lett.* **93**, 036802 (2004).
 - [11] J. Kasprzak *et al.*, *Nature (London)* **443**, 409 (2006).
 - [12] S. Christopoulos *et al.*, *Phys. Rev. Lett.* **98**, 126405 (2007).
 - [13] I. D’Amico *et al.*, *Phys. Status Solidi B* **234**, 58 (2002); X. Li *et al.*, *Science* **301**, 809 (2003); B. Lovett *et al.*, *Phys. Lett. A* **315**, 136 (2003); F. Rossi, *IEEE Trans. Nanotechnol.* **3**, 165 (2004).
 - [14] A. High *et al.*, *Science* **321**, 229 (2008).
 - [15] A. O. Govorov, S. E. Ulloa, K. Karrai, and R. J. Warburton, *Phys. Rev. B* **66**, 081309(R) (2002).
 - [16] L. Dias da Silva, S. Ulloa, and A. Govorov, *Phys. Rev. B* **70**, 155318 (2004).
 - [17] L. Dias da Silva, S. Ulloa, and T. Shahbazyan, *Phys. Rev. B* **72**, 125327 (2005).
 - [18] M. Grochol and R. Zimmermann, *Phys. Rev. B* **76**, 195326 (2007).
 - [19] *Handbook of Mathematical Functions*, edited by M. Abramovitz and I. A. Stegun (Dover, New York, 1972), 9th ed.
 - [20] Here we study $\mu = 1$, but we have checked that F remains zero at $\Phi = 0.5$ and large u_0 down to $\mu = 1/10$.
 - [21] A. V. Chaplik, *Pis'ma Zh. Eksp. Teor. Fiz.* **62**, 885 (1995) [*JETP Lett.* **62**, 900 (1995)]; R. A. Römer and M. E. Raikh, *Phys. Rev. B* **62**, 7045 (2000).
 - [22] A. Maslov and D. Citrin, *Phys. Rev. B* **67**, 121304(R) (2003).
 - [23] In real systems, nonradiative decay due to disorder and similar effects will open a small gap (assuming a fairly clean system at low temperatures to keep the gap small) so that transitions between optically dark and light states are possible for adiabatic changes in u_0 .
 - [24] A. Lorke *et al.*, *Microelectron. Eng.* **47**, 95 (1999); A. Lorke *et al.*, *Phys. Rev. Lett.* **84**, 2223 (2000); R. J. Warburton *et al.*, *Nature (London)* **405**, 926 (2000); M. Bayer *et al.*, *Phys. Rev. Lett.* **90**, 186801 (2003).